arXiv:nucl-ex/0508011v3 10 Sep 2006

Exclusive Measurements of $pd \rightarrow^3 He \; \pi\pi$: the ABC Effect Revisited

M. Bashkanov[a], D. Bogoslawsky[b], H. Calén[c], F. Cappellaro[d], H. Clement[a], L. Demiroers[e],
C. Ekström[c], K. Fransson[c], J. Greiff[c], L. Gustafsson[d], B. Höistad[d], G. Ivanov[b], M. Jacewicz[d],
E. Jiganov[b], T. Johansson[d], O. Khakimova[a], M.M. Kaskulov[a], S. Keleta[d], I. Koch[d], F. Kren[a],
S. Kullander[d], A. Kupść[c], A. Kuznetsov[b], P. Marciniewski[c], R. Meier[a], B. Morosov[b], W. Oelert[f],
C. Pauly[e], Y. Petukho[b], A. Povtorejko[b], R.J.M.Y. Ruber[c], W. Scobel[e], T. Skorodko[a], B. Shwartz[g],
V. Sopov[h], J. Stepaniak[i], V. Tchernyshev[h], P. Thörngren-Engblom[d], V. Tikhomirov[b], A. Turowiecki[j],
G.J. Wagner[a], M. Wolke[d], A. Yamamoto[k], J. Zabierowski[i], and J. Zlomanczuk[d]

[a]Physikalisches Institut der Universität Tübingen, D-72076 Tübingen, Germany

[b]Joint Institute for Nuclear Research, Dubna, Russia

[c]The Svedberg Laboratory, Uppsala, Sweden

[d]Uppsala University, Uppsala,Sweden

[e]Hamburg University, Hamburg, Germany

[f]Forschungszentrum Jülich, Germany

[g]Budker Institute of Nuclear Physics, Novosibirsk, Russia

[h]Institute of Theoretical and Experimental Physics, Moscow, Russia

[i]Soltan Institute of Nuclear Studies, Warsaw and Lodz, Poland

[j]Institute of Experimental Physics, Warsaw, Poland

[k]High Energy Accelerator Research Organization, Tsukuba, Japan

Exclusive measurements of the reactions $pd \rightarrow {}^3\text{He} \; \pi^+\pi^-$ and $pd \rightarrow {}^3\text{He} \; \pi^0\pi^0$ have been carried out at $T_p = 0.893$ GeV at the CELSIUS storage ring using the WASA detector. The $\pi^+\pi^-$ channel evidences a pronounced enhancement at low invariant $\pi\pi$ masses - as anticipated from previous inclusive measurements of the ABC effect. This enhancement is seen to be even much larger in the isoscalar $\pi^0\pi^0$ channel. The differential distributions prove this enhancement to be of scalar-isoscalar nature. $\Delta\Delta$ calculations give a good description of the data, if a boundstate condition is imposed for the intermediate $\Delta\Delta$ system.

About 40 years ago first measurements onto the double-pionic fusion of protons and deuterons to ^{3}He particles led to a big surprise. In the momentum spectra of the ^{3}He particles detected by a magnetic spectrometer Abashian, Booth and Crowe [1] found an intriguing excess of strength close to the $\pi\pi$ threshold. Follow-up measurements of this group suggested this enhancement to be of isoscalar $I_{\pi\pi} = 0$ nature, since corre-sponding measurements on the isovector $\pi^+\pi^0$ channel in $pd \rightarrow {}^3$HX yielded a much smaller cross section. Hence it has been speculated, whether some unknown isoscalar resonance (like, e.g., the σ meson) could be the origin of the observed enhancement. Later on the effect, meanwhile referred to as ABC effect after the initials of the original authors and interpreted as $\Delta\Delta$ excitation [2], was confirmed in much more detailed studies

1

at Saclay [3], even on other nuclear systems [4,5] - though in all cases by inclusive single-arm magnetic spectrometer measurements detecting solely the nuclear recoil particle.

The first exclusive measurements of the $pd \rightarrow$ ^{3}He $\pi^+\pi^-$ reaction have been carried out recently at CELSIUS [6] very close to threshold and at COSY-MOMO [7] near threshold. Whereas in the first case the very limited statistics does not permit any definite conclusions, the MOMO data clearly show a shift of strength towards high invariant $\pi^+\pi^-$ masses $M_{\pi^+\pi^-}$ as compared to phase space distributions. Though this finding near threshold is in contrast to the ABC effect observed at much higher energies, it coincides with that in $pp \rightarrow pp\pi^+\pi^-$ [8], where the close-to-threshold data are in accordance with excitation and decay of the Roper resonance.

In order to shed more light on the nature of the ABC effect we have carried out exclusive measurements of the reactions $pd \rightarrow$ ^{3}He π^0, ^{3}He $\pi^0\pi^0$ and ^{3}He $\pi^+\pi^-$ at $T_p = 0.893$ GeV using the WASA detector [9] with the deuterium pellet target system at the CELSIUS storage ring. The energy chosen corresponds to the one, where the maximum ABC effect has been observed [3]. The detector has nearly full angular coverage for the detection of charged and uncharged particles. The forward detector consists of a thin window plastic scintillator hodoscope at the exit of the scattering chamber, followed by straw tracker, plastic scintillator quirl and range hodoscopes, whereas the central detector comprises in its inner part a thin-walled superconducting magnet containing a minidrift chamber for tracking and in its outer part a plastic scintillator barrel surrounded by an electromagnetic calorimeter consisting of 1012 CsI (Na) crystals.

^{3}He particles have been detected in the forward detector and identified by the ΔE-E technique using corresponding informations from quirl and range hodoscope, respectively. In order to suppress the vast background of fast protons and other minimum ionizing particles already on the trigger level, appropriate ΔE thresholds have been set on the window hodoscope acting as a first level trigger. Fig. 1, top, shows the ΔE-E scatterplot of the events registered in the forward
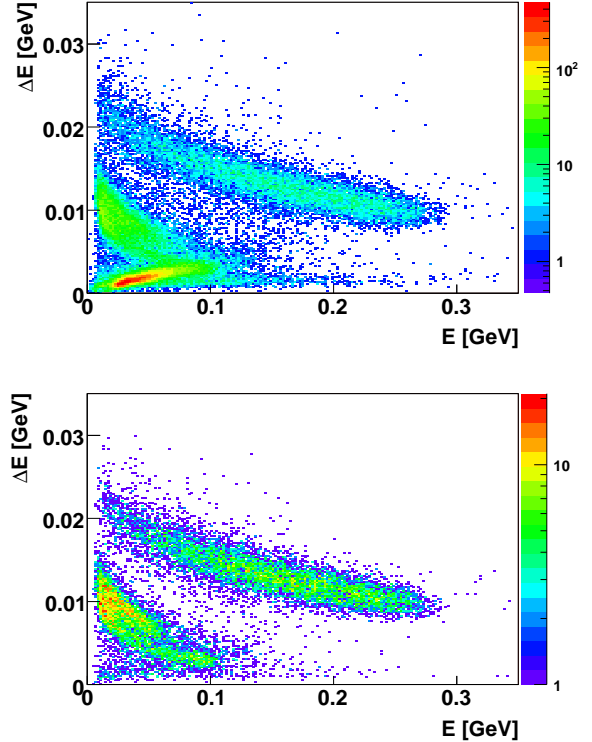

Figure 1. ΔE-E scatterplot for particles stopped in the forward detector, on top without any constraints, at bottom with the constraint of an identified $\pi^+\pi^-$ or $\pi^0\pi^0$ pair in the central detector. Here ΔE and E denote the energy loss in the third layer of quirl and range hodoscope, respectively. The upper band in the plots shows the recorded ^{3}He particles, whereas the lower band contains mainly protons and deuterons. Note also that due to the constraint $\Theta_{^3He}^{cm} \leq 90°$ only ^{3}He particles with $E \geq 0.1$ GeV are taken for the further analysis.
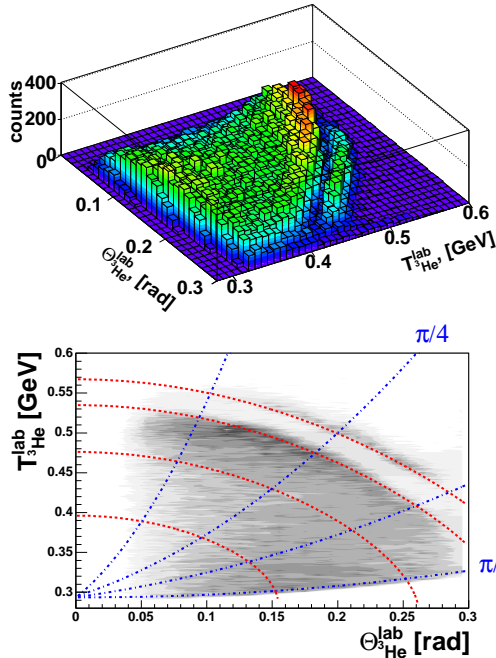
Figure 2. 3D and contourplots of lab angle $\Theta_{^3He}^{lab}$ versus lab energy $T_{^3He}^{lab}$ for ^3He particles measured in the forward detector. The dash-dotted lines give $\Theta_{^3He}^{cm} = 22.5°, 45°, 67.5°, 90°$. The dashed lines indicate the contours of missing masses $MM_{^3He} = 0.135, 0.27, 0.4, 0.5$ GeV

detector. The ^3He band is clearly separated from that for deuterons and protons.

Charged pions and gammas (from π^0 decay) have been detected in the central detector. This way the full four-momenta have been measured for all particles of an event allowing thus kinematic fits with 4 overconstraints in case of $\pi^+\pi^-$ production and 6 overconstraints in case of $\pi^0\pi^0$ production. Fig.1, bottom, shows the ΔE-E scatterplot for events, which contain a pion pair identified in the central detector. There is practically no background any longer beneath the ^3He band.

In order to facilitate comparison with the previous inclusive measurements [3] we display in Fig.

2 lego and contour plots of lab angle versus lab energy of the ^3He particles detected in the forward detector - before kinematic fit and any demand on other particles in the event. Whereas for single π^0 production ^3He particles have been registered only in a very limited angle and energy range of phase space, the ^3He particles stemming from $\pi\pi$ production have been detected over the full kinematical range up to ^3He angles $\Theta_{^3He}^{cm} \leq 90°$. Since we demand the ^3He particles to reach the range hodoscope they need to have kinetic energies of more than 200 MeV in order to be registered and savely identified. Hence for ^3He cms angles much larger than $90°$ the phase space is no longer fully covered in our measurement. In order to avoid extrapolations we introduce therefore the $90°$ cut.

In Fig. 2 the band for single π^0 production is seen to be well separated from the continuum for $\pi\pi$ production. Also immediately evident is a large accumulation of events near the kinematical limit for $\pi\pi$ production, i.e. in the region corresponding to small invariant $\pi\pi$ masses. Since the detector efficiency is approximately constant over the corresponding phasespace region in Fig.2, this feature obviously is in accord with a strong ABC enhancement present in these data. In fact, if we divide Fig. 2 into angular bins, then we obtain spectra in resemblance of those measured at Saclay [3]. As an example we show in Fig. 3 the ^3He momentum spectrum for the angular bin $7° \leq \Theta_{^3He}^{lab} \leq 8°$. The rise at small momenta - corresponding to large missing masses - in the inclusive spectrum can be associated with $\pi\pi\pi$ production (dash-dotted histogram in Fig.3) production and $I_{\pi\pi} = 1$ contributions as will become evident from the analysis of the exclusively measured data.

Next we demand that the ^3He particles are accompanied with 2 or 4 gammas from π^0 decay or a $\pi^+\pi^-$ pair registered in the central detector. The completeness of the events is checked by appropriate missing mass conditions. Having now also the four-momenta of the accomponying particles the selected events are overcomplete and kinematical fitting with 4 to 6 overconstraints can be applied. To obtain further information on the $\pi\pi$ production process we next consider differential observables after correction of the data for acceptance
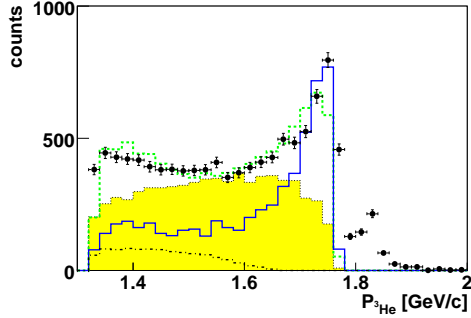
Figure 3. ^{3}He momentum spectrum for the angular bin $7° \leq \Theta_{^3He}^{lab} \leq 8°$ (not corrected for detector efficiency). The data points represent the inclusively measured spectrum for comparison with the Saclay data [3]. The shaded histogram displays the phase space for $\pi\pi$ production normalized as to touch the data as in Ref.[3]. The dash-dotted histogram shows the phase space calculation for $\pi\pi\pi$ production. The dashed histogram represents conventional $\Delta\Delta$ calculations normalized to the data, whereas the solid histogram shows the same calculations with a boundstate condition for the $\Delta\Delta$ system included.

and efficiency. The absolute normalisation of the $\pi\pi$ data is done by normalizing our ^{3}He π^0 data to those from Saclay measurements [10] at neighboring energies. This gives a total cross section of 2.8 (3) μb for the $\pi^0\pi^0$ production and 5.1 (5) μb for the $\pi^+\pi^-$ production. The quoted uncertainties being more than twice the purely statistical ones constitute a very conservative estimate of systematic uncertainties particularly in the absolute efficiency of the detector based on Monte Carlo simulations of the detector performance.

Note that the $\pi\pi$ production cross section is considerably larger than that for single π^0 production (2.7 μb, averaged value from Ref.[10]) as already apparent from Fig. 2. In the free NN system at corresponding energies π^0 production is larger than $\pi^0\pi^0$ production by more than an order of magnitude. The strong suppression of
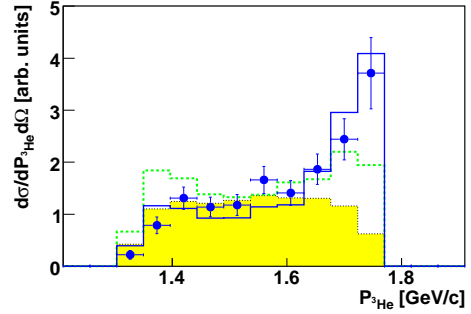

Figure 4. The same as Fig.3, but now for the exclusively measured and efficiency corrected $\pi^0\pi^0$ channel.

single π^0 production here is due to the constraint of having all nucleons in the exit channel fused to ^{3}He.

As mentioned before we cover the full kinematical range of $\pi\pi$ production only for $\Theta_{^3He}^{cm} \leq 90°$. Hence we plot observables in the following only for this kinematical region. If the ^{3}He angular distributions indeed are symmetric about $90°$ as indicated in the Saclay measurements [3], then our data in fact do contain the complete information over the full phase space. The numbers quoted above for the total cross sections actually are derived under this assumption.

Fig. 4 shows the ^{3}He momentum distribution for the same angular slice as in Fig. 3, however, selecting now only the exclusively measured $\pi^0\pi^0$ channel. We see that the relative enhancement at high momenta has strongly increased, whereas the rise at low momenta has disappeared. We note that already in Ref. [5] it had been suggested that the low-momentum rise in the inclusive spectra might be due to $\pi\pi\pi$ rather than $\pi\pi$ production.

Figs. 5 and 6 display the differential distributions for the invariant masses $M_{\pi\pi}$ and $M_{^3He\,\pi}$ as well as angular distributions for $\delta_{\pi\pi}$, the opening angle between the two pions, for the angle of the total momentum of $\pi\pi$ system $\Theta_{\pi\pi}^{cm} = -\Theta_{^3He}^{cm}$ - all

in the overall cms - and for $\Theta_\pi^{\pi\pi}$, the pion angular distribution in the $\pi\pi$ subsystem (Jackson frame), which is shown both for the full mass region (circles) and for $M_{\pi\pi} < 0.34$ GeV (squares). The shaded areas in these plots give the pure phase space distributions. Note that for an (unpolarized) three-body reaction there are only 4 independent observables.

As expected from the discussion of Figs. 1 - 4 we see a strong enhancement in $M_{\pi^0\pi^0}$ at low masses towards threshold. In $M_{\pi^+\pi^-}$ we see such an enhancement, too, however of considerably smaller size. Since low invariant masses belong to $\pi\pi$ pairs with small relative momentum, such pairs must move essentially in parallel both in lab and overall cms thus having a small opening angle $\delta_{\pi\pi} \to 0$ as indeed is borne out in our data for $\delta_{\pi\pi}$ (Fig. 6). The $M_{^3He\,\pi}$ spectra exhibit clear signatures of Δ excitation in the course of the reaction process as anticipated by $\Delta\Delta$ calculations.

The $\Theta_{^3He}^{cm}$ angular dependence is similar to the Saclay results (Figs. 20 and 21 in [3]) though in detail somewhat flatter. However, at Saclay only the angular dependence of the visible enhancement (ABC peak) in the momentum spectra was looked at.

For $\Theta_\pi^{\pi\pi}$ we obtain a slightly non-flat angular distribution in the $\pi^0\pi^0$ channel. For $M_{\pi\pi} < 0.34$ GeV, i.e. the region of the enhancement, the $\Theta_\pi^{\pi\pi}$ distribution turns out, however, to be flat in accordance with pure s-waves, which means that the enhancement is of scalar nature. Note that, since the two π^0 cannot be distinguished, the angular distribution has to be symmetric about 90° by construction. In order to treat the $\pi^+\pi^-$ channel on the same footing we also sort the charged pions independently of their charge into the $\Theta_\pi^{\pi^+\pi^-}$ spectrum symmetrizing thus this spectrum, too.

Since the initial deuteron has isospin 0, whereas proton and ^{3}He have isospin 1/2, the reaction acts as an isospin filter and the $\pi\pi$ pair can only be in an $I_{\pi\pi} = 0$ or 1 state - in case of $\pi^0\pi^0$ even uniquely in $I_{\pi\pi} = 0$ due to Bose symmetry. From previous $pd \to {}^3H\ \pi^+\pi^0$ measurements [1,3], where $I_{\pi\pi} = 1$ solely, the isovector contribution in $pd \to {}^3$He $\pi^+\pi^-$ has been deduced to be smaller by roughly an order of magnitude using isospin relations between both channels. In addi-
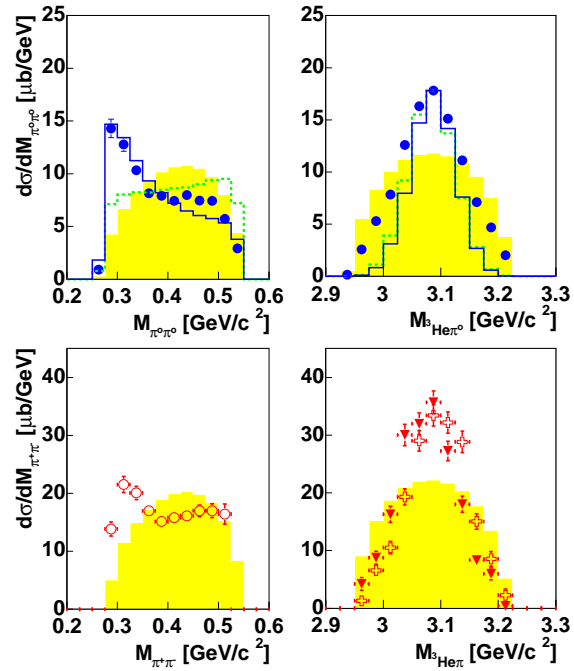

Figure 5. Differential cross sections for the distributions of the invariant masses $M_{\pi\pi}$ (left) and $M_{^3He\,\pi}$ (right, with filled triangles for $M_{^3He\,\pi^-}$ and open crosses for $M_{^3He\,\pi^+}$) . Top: $pd \to {}^3$He $\pi^0\pi^0$, bottom: $pd \to {}^3$He $\pi^+\pi^-$. The shaded areas show the phase space distributions for comparison. Solid and dashed curves denote $\Delta\Delta$ calculations with and without boundstate condition.

tion Bose symmetry necessitates the two pions in the isovector state to be in relative p-wave, which in turn is suppressed at small invariant masses. Therefore the ABC enhancement has been assigned to be of isoscalar nature. On the other hand an $I_{\pi\pi} = 1$ contribution in the $\pi^+\pi^-$ channel should show up at large invariant masses. To investigate this point in more detail we plot both distributions on top of each other in Fig. 7 and divide the $\pi^+\pi^-$ cross section by a factor of two in order to account for the isospin factor between both channels in case of $I_{\pi\pi} = 0$. (Actually this
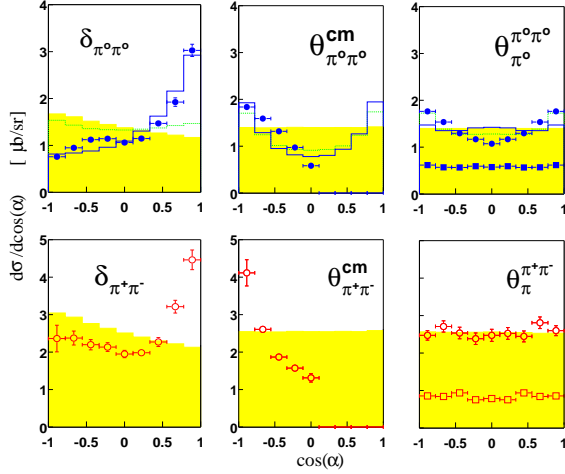
Figure 6. Angular distributions of the opening angle $\delta_{\pi\pi}$ between the two pions, the angle of the total momentum of the $\pi\pi$ system $\Theta^{cm}_{\pi\pi} = -\Theta^{cm}_{^3He}$ - all in the overall cms - as well as the pion angle $\Theta^{\pi\pi}_{\pi}$ in the $\pi\pi$ subsystem (Jackson frame). For the latter the data are plotted also with the constraint $M_{\pi\pi} < 0.34$ GeV. Top: $pd \rightarrow {}^3$He $\pi^0\pi^0$, bottom: $pd \rightarrow {}^3$He $\pi^+\pi^-$. For the meaning of symbols and curves see caption of Fig. 5.

factor needs still to be corrected for the different reaction thresholds of both channels due to the different masses of charged and neutral pions. This kinematical correction is substantial at incident energies near the reaction threshold [6], however close to unity at our energy far above threshold, where the cross section saturates.) We then see that $\sigma(\pi^+\pi^-)/2 \approx \sigma(\pi^0\pi^0)$ in the region 320 MeV $\leq M_{\pi\pi} \leq$ 400 MeV and somewhat larger beyond. If we assign this surplus to the $I_{\pi\pi} = 1$ contribution then we end up with 0.6 μb for the isovector part. The exact value, however, depends strongly on the relative normalizations of $\pi^+\pi^-$ and $\pi^0\pi^0$ channels. Accounting for their uncertainties given above we could have an isovector contribution as large as 1 μb in support of the findings in the inclusive measurements [1,3].
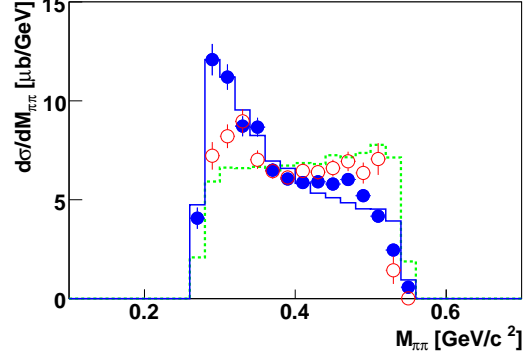

Figure 7. Comparison of the $M_{\pi\pi}$ distribution for $\pi^0\pi^0$ (full symbols) and $\pi^+\pi^-$ (open symbols) channels. The chosen binning reflects the experimental resolution. For easy comparison the $\pi^+\pi^-$ cross section has been divided by a factor of two - the isospin factor relating both channels in the isoscalar case. For the meaning of the curves see caption of Fig. 5.

Coming back to the low-mass region we see (Fig. 7) that strength starts to build up towards low masses in $M_{\pi^+\pi^-}$ until it gets cut off by the $\pi^+\pi^-$ threshold. Due to the 9 MeV lower $\pi^0\pi^0$ threshold, the strength can continue growing towards smaller masses in the $\pi^0\pi^0$ channel. So the main discrepancy between both channels in their low-mass behavior may possibly be associated with the different thresholds, which in turn arise from the different $\pi^\pm$ and π^0 masses and the isospin breaking residing in them. Coulomb effects within the $\pi^+\pi^-$ system can be estimated by the Gamov factor [11] giving a 3% effect at $M_{\pi^+\pi^-} = 0.3$ GeV, which is within the uncertainties of the data and small compared to the discrepancies between $M_{\pi^+\pi^-}$ and $M_{\pi^0\pi^0}$ spectra. Coulomb effects between the $\pi^+\pi^-$ pair and the ^{3}He nucleus could be somewhat larger due to the doubly charged nucleus, but have not been calculated to our knowledge.

We have not yet discussed possible reasons for the observed low-mass enhancement as it man-

ifests itself particularly well in the $M_{\pi^0\pi^0}$ spectrum as the clean isoscalar case. $\Delta\Delta$ calculations [2] for the isoscalar channel, which were thought to provide an explanation for the ABC effect on basis of inclusively measured spectra, give a modest double-hump structure (relative to phase space) in $M_{\pi\pi}$, which obviously is not supported any longer by the new exclusively measured data. A double-hump structure appears to be an important feature of $\Delta\Delta$ excitations, since to our knowledge all calculations to this issue for bound [12,13] nuclear systems in the final state predict such a behavior. Indeed, it has been demonstrated in the very basic and pedagogical paper of Risser and Shuster [14] that the $\Delta\Delta$ amplitude produces this structure by favoring the configurations with the two pions moving either in parallel (low-mass peak) or in antiparallel (high-mass peak), while the two nucleons get confined in the final nuclear bound state. In order to demonstrate this situation we have carried out $\Delta\Delta$ calculations along the lines of Ref.[14] including in addition appropriate angular dependences for the Nπ system in the Δ state. These calculations are shown in Figs. 3 - 7 by the dashed histograms. They, indeed, describe amazingly well the inclusively measured ^{3}He momentum spectra, however, are at variance with the exclusive data for momentum and $M_{\pi\pi}$ spectra. Note that these calculations, though creating big high- and low-momentum enhancements in the momentum spectra, lead to enhancements in $M_{\pi\pi}$, which look quite modest there due to the parabolic shape of the phase space distribution in this spectrum. It has been shown [13] that this double-hump structure gets strongly enhanced in calculations, which account for ρ exchange and short range correlations in addition to π exchange.

Since obviously calculations, which predict a pronounced low-mass enhancement in $M_{\pi\pi}$, also predict an even larger high-mass enhancement, which however is absent in the data for the isoscalar channel, an important piece appears to be missing in such calculations. In the basic picture presented in Ref.[14] this means that the configuration with the two pions moving in antiparallel obviously is suppressed by some reason, e.g., if the two Δ are hindered in their relative motion.

In this case, since the two nucleons of the two Δ are already confined by the nuclear boundstate condition, also the two pions are forced to minimum relative motion. Qualitatively this has the same effect in $M_{\pi\pi}$ as a strong $\pi\pi$ final state interaction originally introduced for the explanation of the ABC effect [1]. Indeed, if we impose such a condition for a quasi-bound $\Delta\Delta$ system in the $\Delta\Delta$ calculations by a simple Gaussian formfactor, then we can obtain a reasonable description of all data for the isoscalar $\pi^0\pi^0$ channel (Figs. 4 - 7, solid histograms). We note that there are quark model based calculations, which indeed predict bound $\Delta\Delta$ states [15].

Another possibility might be chiral restoration [16] [17] or other dynamic [18] effects in the nuclear medium as observed, e.g., in $\pi A \to \pi\pi X$ [19] [20] and $\gamma A \to \pi\pi X$ [21] reactions, or a resonance-like phenomenon near $\pi\pi$ threshold, which - since not observed in reactions on a single nucleon - would need to be associated with the NN system. Such a phenomenon has been noted, e.g., in Refs. [22,23].

Summarizing, the first exclusive data on $pd \to ^3$He $\pi^0\pi^0$ and $pd \to ^3$He $\pi^+\pi^-$ in the ABC region reveal a strong enhancement in the low $M_{\pi\pi}$ region - in the $\pi^0\pi^0$ channel being much larger than in the $\pi^+\pi^-$ channel. From the data we see that this enhancement is of scalar-isoscalar nature and hence shows up especially pronounced in the $\pi^0\pi^0$ channel. The reason for the low-mass enhancement appears still to be an unsettled problem. Ideas presented include medium effects or some unknown phenomenon associated with the NN-system - or possibly a $\Delta\Delta$ mechanism substantially different from what has been assumed previously and possibly connected with a quasi-bound $\Delta\Delta$ system.

8

REFERENCES

1. N. E. Booth, A. Abashian, K. M. Crowe, Phys. Rev. Lett. **7**, 35 (1961); **5**, 258 (1960); PR **132**, 2296ff (1963)

2. J. C. Anjos, D. Levy, A. Santoro, Nucl. Phys. **B67**, 37 (1973)

3. J. Banaigs et al., Nucl. Phys. **B67**, 1 (1973)

4. see; e.g., R. Wurzinger et al., Phys. Lett. **B445**, 423 (1999); for a review see A. Codino and F. Plouin, LNS/Ph/94-06

5. F. Plouin, P. Fleury, C. Wilkin, Phys. Rev. Lett. **65**, 690 (1990)

6. M. Andersson et al., Phys Lett. **B485**, 327 (2000)

7. F. Bellemann et al., Phys Rev. **C60**, 061002(R) (1999)

8. W. Brodowski et al., Phys. Rev. Lett. **88**, 192301 (2002); J. Pätzold et al., Phys. Rev. **C67**, 052202(R) (2003)

9. J. Zabierowski et al., Phys. Scripta **T99**, 159 (2002)

10. J. Banaigns et al., Phys. Lett. **45B**, 394 (1973)

11. I. Juricic et al., Phys. Rev. **D39**, 1 (1989)

12. see, e.g., A. Gardestig, G. Fäldt, C. Wilkin Phys. Rev. **C59**,2608 (1999) and Phys. Lett. **B421**, 41 (1998); C. A. Mosbacher, F. Oster-feld, nucl-th/990364

13. L. Alvarez-Ruso,Phys. Lett. **B452**, 207 (1999) and PhD thesis, Univ. Valencia 1999

14. T. Risser and M. D. Shuster, Phys. Lett. **43B**, 68 (1973)

15. J. Ping, H. Pang, F. Wang, T. Goldman,Phys. Rev. **C65**, 044003 (2002), references therein and priv. comm.

16. T. Hatsuda, T. Kunihiro, H. Shimizu, Phys. Rev. Lett. **82**, 2840 (1999)

17. Z. Aouissat et al., Phys. Rev. **C61**, 012202(R) (1999)

18. L. Roca, E. Oset, M. J. Vicente-Vacas, Phys Lett. **B541**, 77 (2002)

19. F. Bonutti et al., Nucl. Phys. **A677**, 213 (2000)

20. A. Starostin et al., Phys. Rev. Lett. **85**, 5539 (2000)

21. J. G. Messchendorp et al., Phys. Rev. Lett. **89**, 222302 (2002)

22. M. Sander, H. V. von Geramb, Phys. Rev. **C56**, 1218 (1997)

23. V. V. Anisovich, V. A. Nikonov, Eur. Phys. J. **A8**, 401 (2000)